

Evolution of coherent islands during strained-layer Volmer-Weber growth of Si on Ge(111)

Arvind Raviswaran, Chuan-Pu Liu, Jaichan Kim, and David G. Cahill

Department of Materials Science and Materials Research Laboratory, University of Illinois, Urbana, Illinois 61801

J. Murray Gibson

Argonne National Laboratory, 9700 South Cass Avenue, Argonne, Illinois 60439

(Received 18 December 2000; published 7 March 2001)

Deposition of Si on Ge(111) at growth temperatures of 450–500°C by molecular beam epitaxy produces high densities ($>10^{11}$ cm $^{-2}$) of small (width ≈ 10 nm) coherent three-dimensional Si islands. At intermediate temperatures, 550–600°C, islands become incoherent with the Ge(111) substrate when their widths exceed ≈ 18 nm. The activation energy for the maximum island density prior to coalescence is ≈ 1.7 eV over a wide temperature range 450–650°C.

DOI: 10.1103/PhysRevB.63.125314

PACS number(s): 68.55.-a, 81.07.-b, 81.10.-h, 81.15.Hi

I. INTRODUCTION

The thermodynamics of heteroepitaxial crystal growth are typically discussed using terminology proposed by Bauer.^{1,2} In the Volmer-Weber (V-W) growth mode, deposition of a heteroepitaxial layer with surface energy greater than 1/2 the work of adhesion creates three-dimensional islands on the substrate;³ in the Stranski-Krastinov (S-K) growth mode, deposition of a *strained* heteroepitaxial layer with low-surface energy forms a wetting layer prior to the appearance of three-dimensional islands. For many years, the nucleation of misfit dislocations was assumed to trigger the formation of three-dimensional islands in S-K growth. Ten years ago, Eaglesham and Cerullo⁴ showed that islands in an S-K system (e.g., Ge deposited on Si) can be fully coherent and that islanding is enabled by elastic deformation of the island and substrate. This fundamental observation—and the possible applications of this growth mode for the synthesis of “quantum dots” for optoelectronics—has stimulated extensive experimental and theoretical research aimed at untangling the complex interplay between strain, surface energy, and mass transport kinetics that determine the size, shape, and areal density of coherent islands in S-K growth.^{5,6}

By comparison, the evolution of coherent islands in Volmer-Weber (V-W) systems is poorly characterized; an extensive literature exists on metal film nucleation on dielectric crystals,² but, in most cases, the large lattice mismatch and large island sizes ensure that the island/substrate interface is incoherent. Early work⁷ demonstrated that coherent Co islands form during heteroepitaxy on Cu(001). Marè *et al.*,⁸ studied the morphology of Si deposited on Ge(111) at room temperature and annealed at high temperatures; they discovered three-dimensional islands for $T_a > 500^\circ\text{C}$. Si/Ge(111) were also studied by scanning tunneling microscopy:⁹ for low deposition rates at $T = 625^\circ\text{C}$, small Si clusters decorate an otherwise smooth surface. But we are unaware of any prior systematic study of the evolution of the densities, sizes, and relaxation of coherent three-dimensional islands in Volmer-Weber crystal growth.

Our scanning tunneling microscopy (STM) and transmission electron microscopy (TEM) data show that high densities of small coherent islands form in the initial stages of Si

growth on Ge(111), and therefore demonstrate that V-W growth is a promising route for the synthesis of epitaxial nanostructures.

II. EXPERIMENTAL DETAILS

Si islands are grown on Ge(111) substrates by molecular beam epitaxy (MBE). The (111) orientation suppresses the formation of stacking-fault defects that are prevalent during growth of tensile-strained layers on (001) surfaces.¹⁰ The supplier specifies the etch-pit density of the Ge(111) wafers as 5×10^3 cm $^{-2}$. We clean Ge(111) substrates by repeated ozone-assisted oxidation and removal of the oxide in water. Samples are In-bonded to a 3 in. diameter Mo sample block, and the final oxide layer is removed in the MBE growth chamber by annealing for 30 min at 450°C.¹¹

We then grow a 40 nm thick Ge buffer layer at 380°C followed by a 40 nm thick Ge_{0.85}Si_{0.15} buffer layer at 500°C. The chamber pressure rises to $\approx 3 \times 10^{-9}$ Torr during deposition. The alloy buffer layer is needed because we have found that the morphology of pure Ge grown by MBE at $T > 450^\circ\text{C}$ is dominated by step-pinning, presumably due to the effects of contamination of the growth surface. The alloy buffer layer enables smooth starting surfaces at the higher temperatures needed for Si island formation. The thickness of the alloy buffer layer is below the theoretical critical thickness for the motion of threading dislocations. Finally, Si islands are grown by adjusting the sample temperature (450–650°C) and depositing Si with a flux of $\approx 1 \times 10^{14}$ cm $^{-2}$ s $^{-1}$. Since a 0.32 nm high step on a Ge(111) surface is composed of two atomic layers (a “bilayer”), we refer to the quantity of Si deposited in units of equivalent bilayers (BL) where 1 BL = 1.5×10^{15} cm $^{-2}$. After deposition, we immediately turn off the substrate heater to begin cooling the sample; the cooling rate is $\approx 2^\circ\text{C s}^{-1}$.

After growth, selected samples are transferred from the MBE chamber to an analysis chamber through a separately pumped UHV transfer line and characterized by STM. TEM is used *ex situ* to determine the density, shape, coherency, and elastic strain relaxation of Si islands. We prepare the

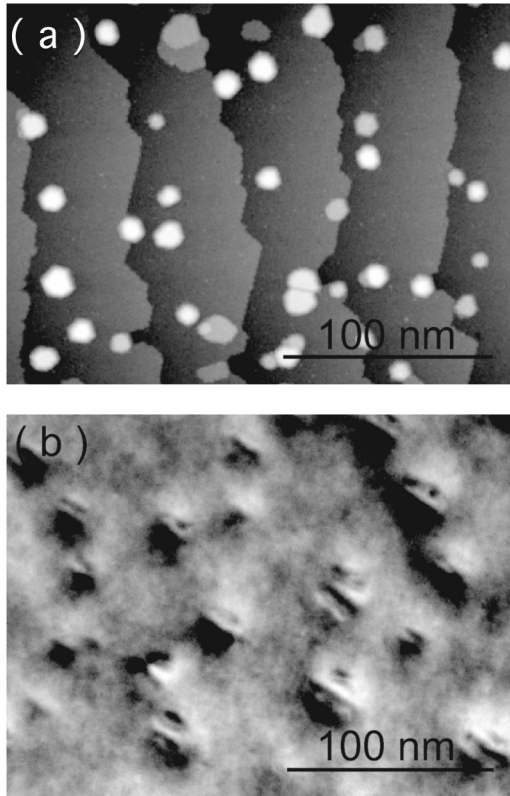


FIG. 1. (a) STM image of coherent islands formed on Ge(111) by the deposition of two equivalent bilayers (BL) of Si at 500°C. (b) Dark-field strain-contrast plan-view TEM images ($g=\langle 220 \rangle$) of islands formed by deposition of 2.8 BL Si on Ge(111) at 550°C.

plan-view foils by mechanical thinning to 30 μm and Ar ion thinning of the backside with the sample holder cooled by liquid nitrogen. We use an exact two-beam diffraction condition for quantitative analysis of strain-contrast.^{12,13} Atomic force microscopy (AFM) is used for island density measurements over large areas. Typically, we find good agreement between STM, TEM, and AFM measurements of island densities.

III. RESULTS AND DISCUSSION

Images of Si islands on Ge(111) are displayed as Fig. 1. The STM data, see Fig. 1(a), reveal fully-formed three-dimensional islands coexisting with a minority of flatter islands that are only 1 or 2 bilayers high. In the TEM data, Fig. 1(b), small coherent islands have the appearance of a “half-moon”; one-half of the island has bright contrast and the other half of the island is dark. Approximately half of the islands are at least partially incoherent at this temperature and coverage. The large lattice mismatch between an incoherent island and the substrate produces closely spaced fringes of light and dark contrast under these imaging conditions.

Figure 2 shows cross-sectional images of coherent and incoherent islands formed at 600°C, the highest deposition temperature at which we have observed coherent islands.

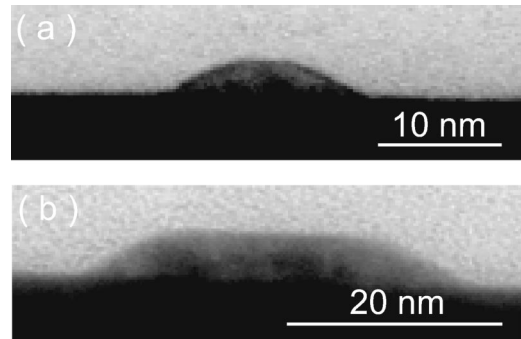


FIG. 2. Cross-sectional TEM images ($\langle 110 \rangle$ zone-axis) of Si islands grown at 600°C by the deposition of 2 BL of Si. (a) An island that is coherent with the substrate; (b) an incoherent island.

The aspect ratio (height h divided by width w) of typical coherent islands is $h/w \approx 0.20$. STM measurements of coherent islands formed at 500° (data not shown) give similar results. While it is tempting to interpret these aspect ratios in terms of the difference in surface energies of Si and Ge, the dependence of the aspect ratio on shape, strain, and surface energy is complex³ and furthermore, since partial Ge termination of the Si island surfaces is likely, we cannot yet estimate the difference in the substrate and island surface energies. In qualitative agreement with the calculation of Johnson and Freund¹⁴ and experiments by LeGoues,¹⁵ the aspect ratios of incoherent islands is smaller, $0.14 < h/w < 0.18$.

Because of the small size of the islands formed at the initial stages of growth, we cannot assign a precise value for the strain relaxation¹² and, therefore, the composition of these islands. Strain relaxation in larger ($w > 15$ nm) coherent islands, however, can be measured accurately using quantitative analysis of the strain-contrast images;^{12,13} the average elastic relaxation of an island is ≈ 0.021 for growth temperatures of 500 and 550°C and ≈ 0.018 at 600°C. These values of the elastic relaxation agree with expectations for a $h/w \approx 0.2$ pure Si island that is coherent with the Ge substrate.¹² The smaller strain relaxation in the 600°C islands may indicate a minor, $< 15\%$, incorporation of Ge at this higher temperature.^{16,17}

Areal densities of islands are summarized in Fig. 3 and demonstrate our principal results: (i) at growth temperatures $T < 500^\circ\text{C}$, high densities, $> 10^{11}$ cm^{-2} , of coherent islands form after a deposition of ≈ 2 BL of Si; (ii) as a function of Si coverage, the island densities increase rapidly due to nucleation and decrease slowly as a result of coalescence; and (iii) the maximum island densities show a strong dependence on temperature, indicating that island nucleation is thermally activated with a large activation energy. The largest island densities we observe, 5×10^{11} cm^{-2} , are a factor of ≈ 5 greater than the highest densities reported for pyramid-shaped islands created by deposition of Ge on Si(001) at a low growth temperature of 300°C,⁶ and comparable to island densities produced at low temperatures in a S-K system with very large lattice mismatch, InAs on Si(001) at 350°C.¹⁸

Figure 4 shows the maximum island density observed at

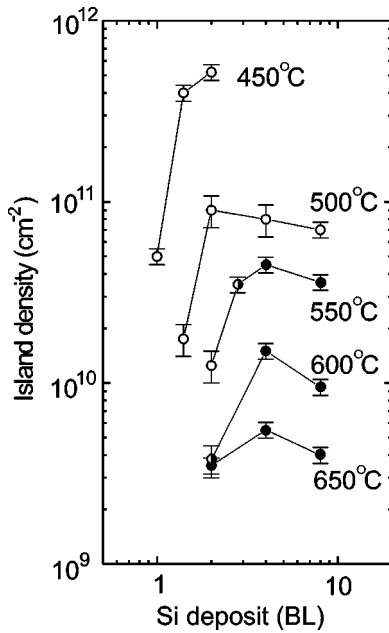


FIG. 3. Evolution of the areal density of Si islands with the amount of Si deposited at growth temperatures 450–650°C. The island densities are measured from a combination of STM, TEM, and AFM images. Error bars indicate the standard deviation of the counting statistics. Open symbols indicate that the majority of Si islands at that temperature and coverage are coherent with the substrate; filled symbols indicate that the majority of islands are incoherent. Only $\approx 1/2$ of the samples were directly characterized for coherency by plan-view TEM; in compiling this figure, we determine the coherency of the remaining samples using the measured island widths and the fact that all of plan-view TEM data are consistent with a coherent-to-incoherent transition at an island width of ≈ 18 nm.

each temperature plotted as a function of reciprocal temperature. We compare our results to rate equation modeling of island nucleation¹⁹ with the assumption of a large critical cluster size, i.e., $i \gg 1$. In this limit, the maximum island density is predicted to be $N_{\max} = (\eta R/\nu) \exp[(E_m + E_f)/k_B T]$, where R is the deposition rate; ν is an atomic-scale attempt frequency; E_m is the activation energy for migration of an adatom; E_f is the formation energy of an adatom;²⁰ and η is parameter of order unity that must be calculated from the theory. We choose $\eta = 0.2$ ¹⁹ and set $\nu = 10^{13}$ Hz. The one remaining parameter, $E_m + E_f$, is varied to fit the data; we find $E_m + E_f = 1.7$ eV. A change of a factor of 2 in the prefactor $\eta R/\nu$ alters this fit by only 0.05 eV. We note that mass transport measurements of $E_m + E_f$ for pure surfaces of Ge(001) and Si(001) give similar values: Ge(001) surface smoothing²¹ shows an activation energy of 1.9 ± 0.25 eV and the activation energy of the step mobility on Si is 1.7 ± 0.1 eV.^{22,23}

But a detailed description of Si island nucleation on Ge(111) is likely to be complex. X-ray photoelectron spectroscopy²⁴ clearly shows the strong propensity for Si deposited on Ge to incorporate below a Ge-rich surface layer. In fact, from our measured island widths, densities, and aspect ratios, we estimate that the first ≈ 1.3 BL of Si deposited

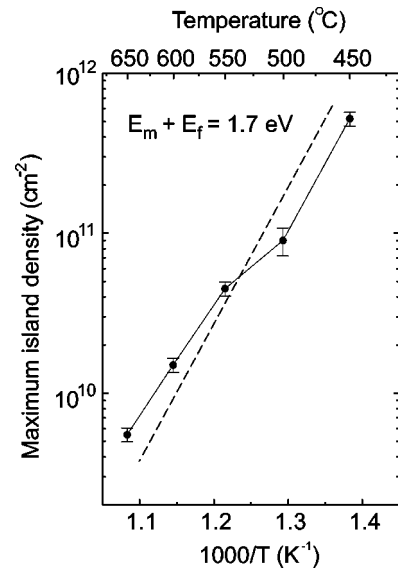


FIG. 4. Dependence of the maximum island density on growth temperature. The dashed line is a predicted maximum island density calculated using rate equation theory for 3D island nucleation in the limit of large cluster size. One free parameter, the sum of the migration energy E_m and the formation energy E_f of adatoms, is adjusted to fit the data; $E_m + E_f \approx 1.7$ eV.

is mostly incorporated into the substrate. Presumably, continued deposition of Si saturates the near surface of the substrate with Si, enabling subsequent nucleation of Si islands, but the continued exchange of Ge and Si atoms at the surface may significantly modify the effective mobility of Si adatoms. As discussed above, the elastic strain relaxation of the islands indicates that the islands are nearly pure Si; we do

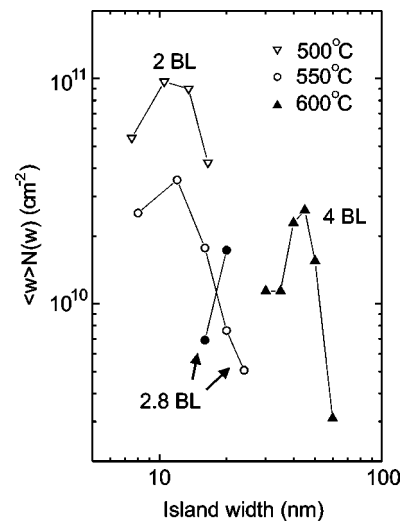


FIG. 5. Island width distribution $N(w)$ (number of islands per unit area per unit width) multiplied by the average island width $\langle w \rangle$ for Si deposition at 500°C (downward pointing triangles), 550°C (circles), and 600°C (upward pointing triangles). Data sets are labeled by the Si coverage in bilayers (BL). Empty symbols show the width distribution of coherent islands and filled symbols are for incoherent islands.

not, however, have any information about the composition of the island or substrate *surfaces*.

The transition between coherent and incoherent islands is more completely characterized by the width distribution data shown in Fig. 5, where we have multiplied the distribution of island widths $N(w)$ by the average width $\langle w \rangle$ of each distribution to obtain a measure with units of areal density. The width distribution of coherent islands overlaps little with the distribution of incoherent islands; the critical width is $w_c \approx 18$ nm at 550°C. We can compare our results to three prior experiments on systems with similar magnitudes of lattice mismatch: hemispherical GaAs islands on Si(001)²⁵ have a smaller critical width, $w_c \approx 12$ nm; the critical width of pyramidal shaped $\text{In}_{0.6}\text{Ga}_{0.4}\text{As}_2$ islands on GaAs(001) is larger, $w_c \approx 30$ nm;²⁶ and for spherical-cap-shaped islands of $\text{In}_{0.5}\text{Ga}_{0.5}\text{As}_2$ on GaAs(001), $w_c \approx 25$ nm.²⁷

Jesser⁷ has provided a relatively simple equation for calculating the equilibrium critical width w_c for the introduction of misfit dislocations at the island/substrate interface; this model builds on the work of Cabrera²⁸ and includes the effects of the elastic relaxation of a hemispherical island. For a substrate and island with similar elastic constants and pure edge dislocations lying in the plane of the interface, $w_c \approx -2b \ln(\pi\epsilon)/\epsilon$, where b is the Burger's vector and ϵ the magnitude of the misfit.⁷ For Si/Ge(111), $b=0.38$ nm, $\epsilon = 0.042$, and this equation predicts $w_c \approx 36$ nm, a factor of 2 larger than our observations. More sophisticated numerical analysis²⁶ of elastic strains and dislocation energies in a spherical-cap-shaped island gives $w_c \approx 24$ nm for the first introduction of 60° dislocations at a (100) interface. The fact

that our (111) surface are a glide plane should enable introduction of pure edge dislocations at the substrate/island interface; in this case, the predicted w_c based on Ref. 26 will be smaller.

Given the close agreement of the measured and calculated w_c ,²⁶ we conclude that the transition between coherent and incoherent islands in the Si/Ge(111) system occurs near equilibrium, i.e., kinetic limitations on dislocation nucleation and motion do not play a significant role, at least at $T > 500^\circ\text{C}$. This behavior, while not surprising, can be contrasted with the behavior of the more widely studied S-K growth of Ge on Si(001). Relatively pure, Ge dome-shaped islands as large as 100 nm in diameter are routinely observed to be fully coherent with Si(001) substrates;¹² nucleation of dislocations^{29,30} in this system is thought to occur only when adjacent islands meet and the stress-concentration³¹ at the island edges increases. Apparently, the stress-concentration at the edges of our Si/Ge(111) islands is sufficient to cause dislocation nucleation even for isolated islands.

ACKNOWLEDGMENTS

We thank D. Jeffers for his assistance with the MBE equipment. This work was supported by National Science Foundation Grant No. DMR-9705440 and the U.S. Department of Energy, Division of Materials Sciences, under Contract No. DEFG02-ER9645439. Sample characterization by TEM, AFM, and SEM used the facilities of the Center for Microanalysis of Materials at the University of Illinois.

¹E. Bauer, Z. Kristallogr. **110**, 372 (1958).

²R. Kern, G. Le Lay, and J. J. Metois, in *Current Topics in Materials Science*, Vol. 3, edited by E. Kaldis (North-Holland, 1979), pp. 130–419.

³P. Müller and R. Kern, J. Cryst. Growth **193**, 257 (1998).

⁴D.J. Eaglesham and M. Cerullo, Phys. Rev. Lett. **64**, 1943 (1990).

⁵I. Daruka, J. Tersoff, and A.-L. Barabási, Phys. Rev. Lett. **82**, 2753 (1999).

⁶D.E. Jesson, M. Kästner, and B. Voigtländer, Phys. Rev. Lett. **84**, 330 (2000).

⁷W.A. Jesser and J.W. Matthews, Philos. Mag. **17**, 461 (1968).

⁸P.M.J. Marèe, K. Nakagawa, F.M. Mulders, J.F. Van der Veen, and K.L. Kavanagh, Surf. Sci. **191**, 305 (1987).

⁹D.-S. Lin, Hawoong Hong, T. Miller, and T.-C. Chiang, Surf. Sci. **312**, 213 (1994); the Si deposition flux used by Lin *et al.* was a factor of 30 smaller than in our experiments.

¹⁰J.E. Van Nostrand, D.G. Cahill, I. Petrov, and J.E. Greene, J. Appl. Phys. **83**, 1096 (1998).

¹¹J.E. Van Nostrand, S.J. Chey, M.-A. Hasan, D.G. Cahill, and J.E. Greene, Phys. Rev. Lett. **74**, 1127 (1995).

¹²C.-P. Liu, J.M. Gibson, D.G. Cahill, T.I. Kamins, D.P. Basile, and R.S. Williams, Phys. Rev. Lett. **84**, 1958 (2000).

¹³C.-P. Liu, P. D. Miller, W. L. Henstrom, and J. M. Gibson, J. Microsc. **199**, 130 (2000).

¹⁴H.T. Johnson and L.B. Freund, J. Appl. Phys. **81**, 6081 (1997).

¹⁵F.K. LeGoues, M.C. Reuter, J. Tersoff, M. Hammar, and R.M. Tromp, Phys. Rev. Lett. **73**, 300 (1994).

¹⁶S.A. Chaparro, J. Drucker, Y. Zhang, D. Chandrasekhar, M.R. McCartney, and D.J. Smith, Phys. Rev. Lett. **83**, 1199 (1999).

¹⁷W.L. Henstrom, C.-P. Liu, J.M. Gibson, T.I. Kamins, and R.S. Williams, Appl. Phys. Lett. **77**, 1623 (2000).

¹⁸P.C. Sharma, K.W. Alt, D.Y. Yeh, and K.L. Wang, Appl. Phys. Lett. **75**, 1273 (1999).

¹⁹J.A. Venables, G.D.T. Spiller, and M. Hanbücken, Rep. Prog. Phys. **47**, 399 (1984).

²⁰More precisely, the term E_f in this expression is the binding energy per atom of a cluster of critical size. In the limit of large critical cluster size $i \gg 1$, the binding energy per atom becomes equivalent to the adatom formation energy; see Ref. 19.

²¹S.J. Chey, J.E. Van Nostrand, and D.G. Cahill, Phys. Rev. Lett. **76**, 3995 (1996).

²²N.C. Bartelt and R.M. Tromp, Phys. Rev. B **54**, 11 731 (1996).

²³J. Chey and D. G. Cahill, in *Dynamics of Crystal Surfaces and Interfaces*, edited by P. M. Duxbury and T. J. Pence (Plenum Press, New York, 1997), p. 59.

²⁴D.-S. Lin, T. Miller, and T.-C. Chiang, Phys. Rev. B **45**, 11 415 (1992).

²⁵R. Hull and A. Fischer-Colbrie, Appl. Phys. Lett. **50**, 851 (1987).

²⁶K. Tillmann and A. Förster, Thin Solid Films **368**, 93 (2000).

- ²⁷S. Guha, A. Madhukar, and K.C. Rajkumar, *Appl. Phys. Lett.* **57**, 2110 (1990).
- ²⁸N. Cabrera, *Surf. Sci.* **2**, 320 (1964).
- ²⁹R. Hull and E.A. Stach, *Curr. Opin. Solid State* **1**, 21 (1996).
- ³⁰U. Jain, S.C. Jain, A.H. Harker, and R. Bullough, *J. Appl. Phys.* **77**, 103 (1995).
- ³¹D.E. Jesson, S.J. Pennycook, J.-M. Baribeau, and D.C. Houghton, *Phys. Rev. Lett.* **71**, 1744 (1993).